Mitochondrially targeted ceramides preferentially promote autophagy, retard cell growth, and induce apoptosis

Qi Hou,[1,*,†] Junfei Jin,[1,†,§] Hui Zhou,[†] Sergei A. Novgorodov,[**] Alicja Bielawska,[†] Zdzislaw M. Szulc,[†] Yusuf A. Hannun,[†] Lina M. Obeid,[,††] and Yi-Te Hsu[2,†]**

Department of Pharmacology,* Institute of Materia Medica, Peking Union Medical College and Chinese Academy of Medical Sciences, Beijing 100050, P R China; Department of Biochemistry and Molecular Biology,[†] and Department of Medicine,**Medical University of South Carolina, Charleston, SC 29425; Research Center of Life Science,[§] University of South China, Hengyang, Hunan 421001, P R China; and Ralph H. Johnson Veterans Affairs Medical Center,[††] Charleston, SC 29401

Abstract **C_6-pyridinium (D-*erythro*-2-*N*-[6′-(1″-pyridinium)-hexanoyl]sphingosine bromide [LCL29]) is a cationic mitochondrion-targeting ceramide analog that promotes mitochondrial permeabilization and cancer cell death. In this study, we compared the biological effects of that compound with those of D-*erythro*-C_6-ceramide, its non-mitochondrion-targeting analog. In MCF7 cells it was found that C_6-pyridinium ceramide preferentially promoted autophagosome formation and retarded cell growth more extensively than its uncharged analog. This preferential inhibition of cell growth was also observed in breast epithelial cells and other breast cancer cells. In addition, this compound could promote Bax translocation to mitochondria. This redistribution of Bax in MCF7 cells could be blocked by the pan-caspase inhibitor zVAD-fmk but via a Bid-independent signaling pathway. Moreover, C_6-pyridinium ceramide-induced translocation of Bax to mitochondria led to mitochondrial permeabilization and cell death. Overall, we show that mitochondrial targeting of C_6-pyridinium ceramide significantly enhances cellular response to this compound.**—Hou, Q., J. Jin, H. Zhou, S. A. Novgorodov, A. Bielawska, Z. M. Szulc, Y. A. Hannun, L. M. Obeid, and Y-T. Hsu. **Mitochondrially targeted ceramides preferentially promote autophagy, retard cell growth, and induce apoptosis. *J. Lipid Res.* 2011.** 52: **278–288.**

Supplementary key words ceramide • Bax • mitochondria

Ceramides are bioactive lipids that affect a wide range of biological processes, such as regulation of cellular proliferation, autophagy, and apoptosis (1, 2). Ceramides can be generated through the action of sphingomyelinase or via the de novo synthetic pathway through the action of ceramide synthases (3). Ceramides generated via sphingomyelin hydrolysis can be further hydrolyzed by ceramidases to form sphingosine, which can then be reacylated via the action of ceramide synthases (CerS [also known as LASS]) to regenerate ceramide species. Additions of sphingomyelinase and short-chained C_2-ceramides were shown to inhibit the proliferation of resting T cells (4).

Ceramides also have been shown to induce cellular autophagy, a process utilized to recycle cellular proteins and damaged organelles. Addition of C_2-ceramide resulted in the accumulation of autophagic vesicles in HT-29 colon cancer cells (5). In addition, treatment of MCF7 breast carcinoma cells with the autophagy inducer tamoxifen elevated ceramide production. Tamoxifen-induced autophagy could be inhibited by myriocin, an inhibitor of the de novo pathway of ceramide synthesis (5).

Ceramides are also well-known inducers of apoptosis (6). The resulting apoptotic process appears to involve the proapoptotic protein Bax. Bax is a member of the Bcl-2 family that plays an important role in apoptosis regulation (7). This protein is primarily soluble in healthy cells (8–11). Upon treatment with a variety of apoptotic stimuli, Bax translocates to mitochondria, where it causes the loss

This research was supported in part by National Institutes of Health Grants NS-40932 (Y-T. H.) and AG-16583 (L. M. O.) and a MERIT Award (L. M. O.) from the Office of Research and Development, US Department of Veterans Affairs. Its contents are solely the responsibility of the authors and do not necessarily represent the official views of the National Institutes of Health or other granting agencies.

Manuscript received 13 October 2010 and in revised form 15 November 2010.

Published, JLR Papers in Press, November 16, 2010
DOI 10.1194/jlr.M012161

Abbreviations: C_6-pyridinium, D-*erythro*-2-*N*-[6′-(1″-pyridinium)-hexanoyl]sphingosine bromide; CerS, ceramide synthase; GFP, green fluorescent protein; MEGM, mammary epithelial growth medium; siRNA, short-interfering RNA; TNF-α, tumor necrosis factor α.

[1] Q. Hou and J. Jin contributed equally to this work.
[2] To whom correspondence should be addressed.
e-mail: hsuy@musc.edu

of mitochondrial membrane potential (8–11) and the release of cytochrome c from mitochondrial intermembrane spaces (12–15). It has been reported that the addition of exogenous C_2- and C_6-ceramides would result in the redistribution of the proapoptotic protein Bax to mitochondria in HL-60 cells and in Bax-transfected DU-145 cells (16). In addition, it has been reported that ultraviolet irradiation could activate sphingomyelinases, resulting in ceramide upregulation and Bax conformational change in HeLa cells (17). Moreover, it has been shown that expression of mitochondrion-targeting bacterial sphingomyelinase could trigger Bax translocation to mitochondria (18).

Currently, two major apoptotic pathways that signal Bax translocation to mitochondria have been identified (19). In the extrinsic pathway, the binding of death ligands such as FAS and tumor necrosis factor-α (TNF-α) to their respective receptors results in the activation of caspase-8. Caspase-8 then cleaves the BH3-only Bid protein, and truncated Bid (tBid) leads to Bax activation and translocation to mitochondria (20–22). In the intrinsic pathway, apoptotic stimuli such as staurosporine and ultraviolet irradiation trigger Bax translocation to mitochondria via mechanisms that are independent of caspase-8 and Bid.

Ceramides can be chemically modified to direct their sequestration to a particular cellular compartment. D-*erythro*-2-*N*-[6′-(1″-pyridinium)-hexanoyl]sphingosine bromide (LCL29) (C_6-pyridinium) ceramide is a positively charged analog of the C_6-ceramide that targets mitochondria and causes mitochondrial permeabilization (23, 24). Its L-*threo* isomer (LCL124) has displayed a potent antitumor effect in human head and neck squamous cell carcinomas (25). As C_6-pyridinium ceramide elicits a number of the above-mentioned biological effects, it is unclear how the mitochondrial targeting of this compound will affect its potency. Here, we show that this positively charged ceramidoid, compared with its neutral counterpart, elicits enhanced proficiency in regulating various cellular processes in MCF7 cells, including cellular growth, autophagy, and apoptosis. In addition, we show that C_6-pyridinium ceramide-induced cell death involves Bax redistribution, independently of Bid.

MATERIALS AND METHODS

Materials

MCF7, MCF10A, MDA-MB-157, and MDA-MB-231 cells were obtained from American Type Culture Collection. LysoTracker Red, fetal bovine serum (FBS), Dulbecco's modified Eagle's medium (DMEM), and tissue culture supplements were from Invitrogen, Inc. FuGENE 6 transfection reagent was from Roche, and Maxiprep kits were from Qiagen. Horseradish peroxidase- and Cy3-conjugated secondary immunoglobulins and enhanced chemiluminescence (ECL) Western blotting detection kit were obtained from Amersham. Anti-Bid and cytochrome c antibodies were from BD Pharmingen. Anti-LC3 antibody was from Santa Cruz Biotechnology. Human LC3 TruClone cDNA was purchased from Origene. Pan-caspase inhibitor zVAD-fmk and a mammary epithelial growth medium (MEGM) kit were purchased from Lonza Corp. Oligonucleotides and transfection reagents used in short-interfering RNA (siRNA) studies were purchased from Dharmacon. A mitochondria isolation kit was from Pierce. All other chemicals were from either Sigma or Fisher Scientific. C_6-pyridinium ceramide (LCL29) and C_6-ceramide were synthesized by the Lipidomics Core facility at Medical University of South Carolina as previously described and were dissolved in dimethyl sulfoxide (24).

Cell culturing

MCF7, MDA-MB-157, and MDA-MB-231 cells were cultured in DMEM supplemented with 10% FBS. MCF10A cells were cultured by using a MEGM kit supplemented with 10% FBS. All cells were maintained in 5% Co_2 at 37°C.

Development of MCF7 cells stably expressing green fluorescent protein-LC3

Human LC3 cDNA was amplified by PCR and cloned into *Hind*III and *Eco*RI sites of the LC3 -EGFP vector (GFP-LC3). To develop stable clones of MCF7 cells expressing GFP-LC3, MCF7 cells were seeded onto 10 cm plates and cultured in DMEM supplemented with 10% FBS. Cells were transfected with 12 μg of C3-GFP-LC3 plasmid with FuGENE transfection reagent. The day after transfection, cells were selected with 0.2 mg/ml G418. After a week of selection, GFP-positive cells were sorted by flow cytometry and maintained in DMEM culture medium in the presence of 0.2 mg/ml G418.

MTT and Trypan blue exclusion assays

Cell growth assay was determined by using an in vitro 3-(4,5-dimethylthiazol-2-yl)-2,5-diphenyltetrazolium bromide (MTT)-based assay kit according to the manufacturer's instructions. Briefly, MCF7, MCF10A, MDA-MB-157, and MDA-MB-231 cells were seeded onto 6-well plates at a density of 6×10^5 cells/ml. After 24 h, cells were incubated with different concentrations of C_6-pyridinium ceramide or C_6-ceramide for specified times. The IC_{50} of each compound was determined from cell growth plots (26). For Trypan blue exclusion assay, MCF7 cells were plated onto 6-well plates (1×10^5 cells/plate) and then treated with 10 μM C_6-pyridinium ceramide or C_6-ceramide for specified times. Cells were then collected and mixed 1:1 (w/v) with Trypan blue dye. Cells that excluded the dye were counted.

Induction of apoptosis by TNF-α, staurosporine, and C_6-pyridinium ceramide

MCF7 or GFP-Bax stable MCF7 cells were plated onto 6-well plates. Cells were then treated with TNF-α, staurosporine, cetylpyridinium bromide, C_6-ceramide, or C_6-pyridinium ceramide. After specified times, cells were either visualized with fluorescence microscopy or subjected to immunofluorescence labeling with anti-Bid or anti-cytochrome c antibody. Subcellular fractionation to prepare cytosolic and heavy membrane fractions from cells treated with these agents was carried out using a mitochondria isolation kit according to the manufacturer's protocol. Resulting protein samples were analyzed by Western blotting with an anti-Bax antibody. To visualize colocalization of Bax with mitochondria, MCF7 cells stably expressing GFP-Bax and mitochondrially-targeted red fluorescent protein (DS-red-mito; 27) were treated with the ceramides for 18 h and then visualized with fluorescence microscopy.

Immunofluorescence labeling and fluorescence microscopy

For immunofluorescence labeling, MCF7 cells were plated onto 6-well plates. Cells were subjected to apoptosis induction with the above-stated agents, in the presence or absence of 50 μM zVAD-fmk, for specified time periods. Both treated and untreated

cells were then washed three times in phosphate-buffered saline (PBS), fixed in 6% paraformaldehyde for 30 min, and permeabilized with a 0.06% saponin solution in PBS for 15 min. Cells were subsequently blocked for 30 min in the blocking buffer containing PBS, 5% FBS, and a 0.06% saponin mixture. Cells were then incubated with 5 μg/ml anti-Bid, or 5 μg/ml anti-cytochrome c antibody diluted in blocking buffer containing a 0.04% saponin mixture for 2 h. Cells were then washed and incubated with 6 μg/ml Cy3-labeled goat anti-rabbit or goat anti-mouse immunoglobulin in the blocking buffer containing a 0.04% saponin solution for an additional 2 h. Cells were then washed with PBS and treated with the antifade reagent. Cells were visualized with an Olympus IX-70 fluorescence microscope using an LCPlanFI 20× objective lens at 1.5× intermediate magnification. Images were acquired with an Optronics DEI-750D digital imaging camera.

Induction of autophagy by ceramide

For LysoTracker staining studies, GFP-Bax stable MCF7 cells were plated onto 6-well plates. Cells were then incubated with 10 μM C_6-pyridinium ceramide or C_6-ceramide for 16 h. Cells were then stained with 0.75 μM LysoTracker Red for 30 min and visualized with an Olympus IX-70 fluorescence microscope. To visualize autophagosome formation, GFP-LC3 stable MCF7 cells were plated onto 6-well plates, treated with C_6-pyridinium ceramide or C_6-ceramide for 16 h, and visualized by fluorescence microscopy. For assessment of the LC3-II-to-LC3-I ratio by immunoblotting, cells were treated with 10 μM C_6-pyridinium ceramide or C_6-ceramide for 18 h. Cell lysates were then analyzed by Western blotting with an anti-LC3 antibody. To determine the level of Beclin-1 in the cell lysates, Western blotting analysis with an anti-Beclin-1 antibody was carried out. The expression level of Beclin-1 was normalized to that of β-actin, using a Scion image program.

SDS-PAGE and Western blotting

SDS-PAGE (12%) and Western blotting analyses were carried out as previously described (28). For immunoblotting analysis, blots were probed with anti-Bax, Bcl-2, and Bcl-X_L (1:10 dilution culture fluid) (9, 28), ATP-synthase β-subunit 9D7 (1:10 dilution culture fluid), anti-Bid (1 μg/ml), anti-LC3 (1 μg/ml), anti-Beclin-1 (1 μg/ml), or anti-β-actin (1 μg/ml) antibody. Immunoblotting and ECL documentation were carried out as previously described (28).

RESULTS

C_6-pyridinium ceramide preferentially mediates autophagy in MCF7 cells

Elevation in ceramide levels has been attributed to an elevation in cellular autophagy (5). To determine the efficacy of short-chained ceramides in promoting autophagosome formation, we treated MCF7 cells with either C_6-ceramide or C_6-pyridinium ceramide for 16 h. Cells were then stained with LysoTracker Red and visualized by fluorescence microscopy. As shown in **Fig. 1A**, a number of cells treated with C_6-pyridinium ceramide displayed LysoTracker Red-stained vesicles. On the other hand, untreated and C_6-ceramide-treated cells showed far fewer stained vesicles. In addition, MCF7 cells stably expressing GFP-LC3 were generated. Cells were then treated with the above-stated compounds for 16 h and visualized by fluorescence microscopy. As shown in Fig. 1B, the cells treated with the positive control tamoxifen displayed numerous GFP-labeled autophagosome vesicles. Similarly, cells treated with C_6-pyridinium ceramide had numerous autophagosome vesicles, albeit fewer than the tamoxifen-treated cells. On the other hand, in untreated and C_6-ceramide-treated cells, GFP-LC3 remained primarily in the cytoplasm.

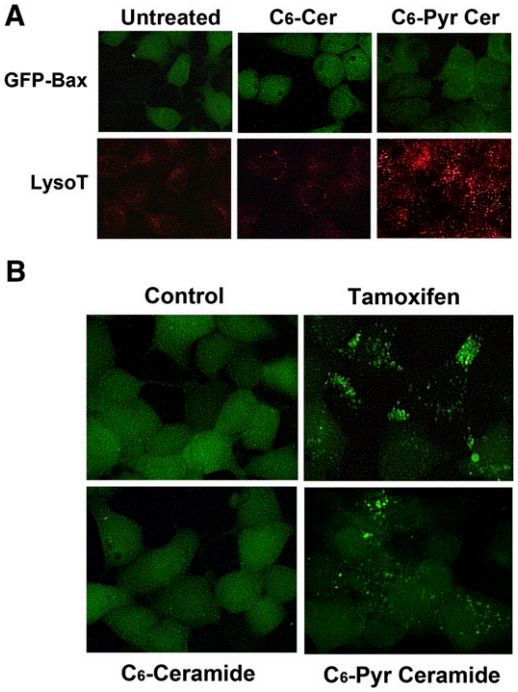

Fig. 1. C_6-pyridinium ceramide (C_6-Pyr-Cer) selectively promotes the formation of autophagosomes. A: MCF7 cells stably expressing GFP-Bax were treated with 10 μM C_6-pyridinium ceramide or C_6-ceramide (C_6-Cer) for 16 h. Cells were then stained with LysoTracker Red (LysoT) and visualized by fluorescence microscopy. B: GFP-LC3-stable MCF7 cells were treated with 50 μM tamoxifen, 10 μM C_6-pyridinium ceramide, or 10 μM C_6-ceramide for 16 h. Cells were then visualized by fluorescence microscopy.

In addition, Western blotting analysis of cell lysates was carried out to determine the LC3-II-to-LC3-I ratio, which serves as an indicator of autophagosome formation. As shown in **Fig. 2A**,, upon treatment with C_6-pyridinium ceramide or tamoxifen, there was an obvious increase in the LC3-II-to-LC3-I ratio, compared with that in untreated and C_6-ceramide-treated cells. We also examined the lysates from MCF10A breast epithelial cells, MDA-MB-137 medullary carcinoma, and MDA-MB-231 breast adenocarcinoma cells. Interestingly, both of the treatments with C_6-ceramide and C_6-pyridinium ceramide resulted in an increase in the LC3-II-to-LC3-I ratio in MDA-MB-231 cells. No LC3 was detected in MCF10A and MDA-MB-137 cell lysates. Moreover, the level of Beclin-1 in MCF7 cells following ceramide treatment was also examined. We found that treatment with C_6-pyridinium ceramide did not appreciably increase the level of Beclin-1 (Fig. 2B, C).

C_6-pyridinium ceramide inhibits cell growth and promotes cell death

To assess the effects of C_6-pyridinium ceramide and C_6-ceramide on cell growth, MCF7 cells were treated with different concentrations of these compounds. At 24 h posttreatment,

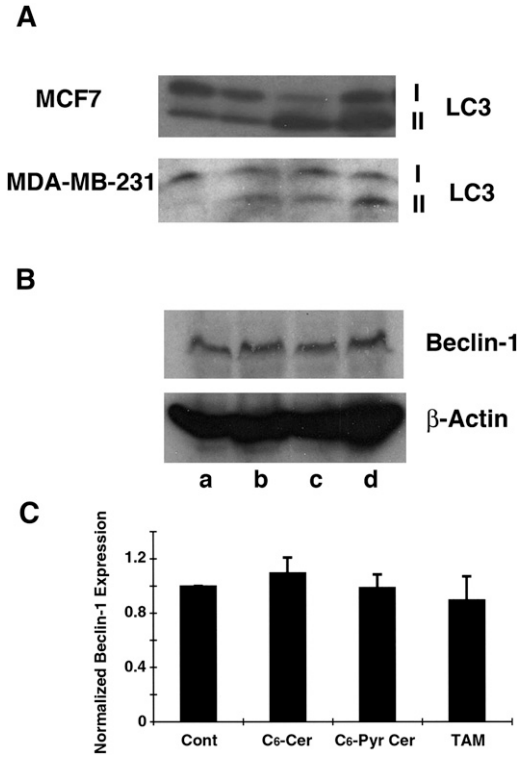

Fig. 2. C_6-pyridinium ceramide (C_6-Pyr-Cer) elevates the ratio of LC3-II/LC3-I without markedly changing the level of Beclin-1. A: MCF7 and MDA-MB-231 cells were treated with 10 μM C_6-ceramide (C_6-Cer), 10 μM C_6-pyridinium ceramide, or 50 μM tamoxifen (TAM), for 16 h. Cell lysates from untreated (lanes a), C_6-ceramide- (lanes b), C_6-pyridinium ceramide- (lanes c), or tamoxifen-treated (lanes d) cells were analyzed by Western blotting with anti-LC3. The positions of LC3-I and -II forms are indicated. B: MCF7 cells lysates from the above treatment were analyzed by Western blotting with anti-Beclin 1 and β-actin antibodies. C: The relative expression levels of Beclin-1 from different treatments were normalized to β-actin and compared with the control untreated sample. Results were averaged from three independent studies.

cells were analyzed using the MTT assay. As shown in **Fig. 3A**, increasing concentrations of C_6-pyridinium ceramide significantly enhanced the inhibition of cell growth. The IC_{50} of this compound was found to be 20 μM compared with an IC_{50} of 80 μM for C_6-ceramide (Fig. 3A). We also monitored cell growth inhibition over time in the presence of 10 μM of these compounds. As shown in Fig. 3B, cell growth inhibition was significantly higher after 24 h treatment with C_6-pyridinium ceramide than with C_6-ceramide. To corroborate the MTT assay results of growth inhibition, Trypan blue exclusion analyses of untreated cells and MCF7 cells treated with 10 μM C_6-ceramide or C_6-pyridinium ceramide were carried out. As shown in Fig. 3C, the number of live cells following C_6-ceramide treatment remained relatively constant over time, whereas the number live cells decreased over time following C_6-pyridinium ceramide treatment. This suggests that in addition to inhibiting cell growth, C_6-pyridinium ceramide may also promote cell death.

In addition to examining effects on MCF7 cells, we also compared the effects of these two compounds on the growth of MCF10A, MDA-MB-157, and MD-MB-231 cells by using the MTT assay. **Figure 4A** shows that increasing concentrations of C_6-pyridinium ceramide significantly enhanced the inhibition of cell growth. The IC_{50}s of these compounds were found to be 52 μM, 4 μM, and 48 μM, respectively, for the above-listed cells. On the other hand, the growth of these cells remained static following C_6-ceramide treatment. We also monitored cell growth inhibition over time in the presence of 10 μM of these compounds. As shown in Fig. 4B, cell growth inhibition and most likely a decrease in cell viability were evident over time for all three cell lines upon C_6-pyridinium ceramide treatment, compared with that with C_6-ceramide treatment.

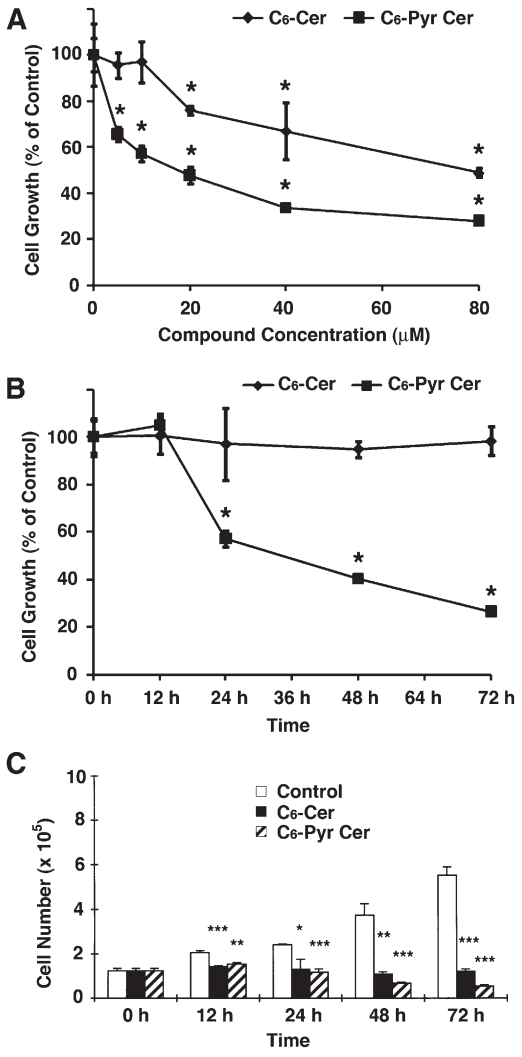

Fig. 3. C_6-pyridinium ceramide (C_6-Pyr-Cer) inhibited MCF7 cell growth in a dose- and time-dependent manner. MCF7 cells were plated onto 6-well plates and treated with different concentrations (0–80 μM) of C_6-pyridinium ceramide or C_6-ceramide (C_6-Cer) for 24 h (A), or with 10 μM of these compounds for various time periods (B). At specified time points, MTT assays were performed. Time-course results were normalized to values from the control cells at the initial time point. C: Control MCF7 cells and cells treated with 10 μM C_6-ceramide or C_6-pyridinium ceramide were collected and stained with Trypan blue to determine the number of live cells at different time points. All results were averaged from three independent studies. Values are means ± SEM. *, $P < 0.05$; **, $P < 0.01$; ***, $P < 0.001$ versus the control.

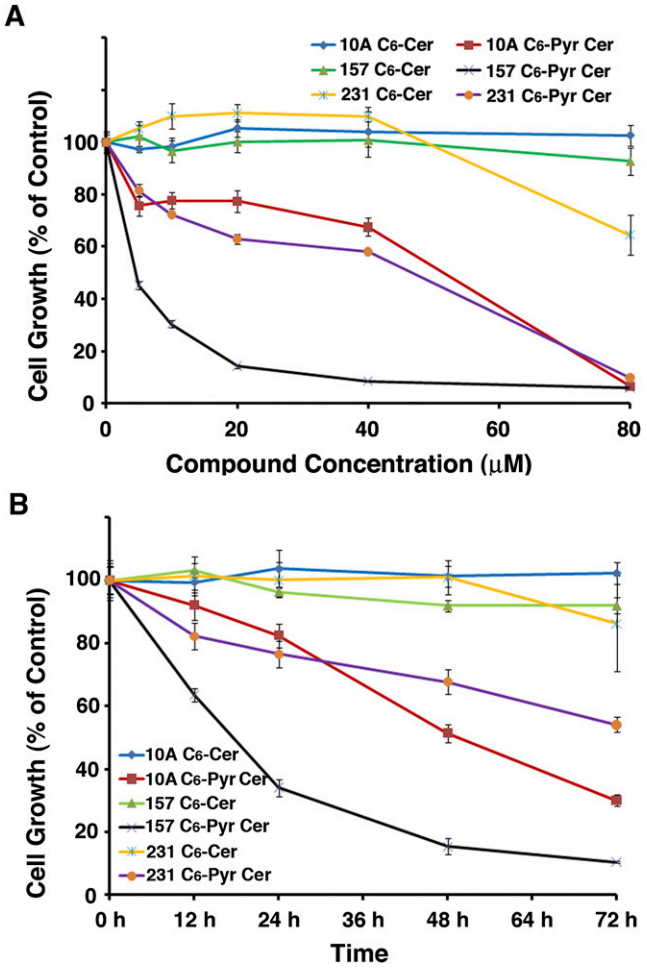

Fig. 4. C_6-pyridinium ceramide (C_6-Pyr-Cer) inhibited growth of various types of cell lines in a dose- and time-dependent manner. MCF10A, MDA-MB-157, and MDA-MB-231 cells were plated onto 6-well plates and treated with different concentrations (0–80 μM) of C_6-pyridinium ceramide or C_6-ceramide (C_6-Cer) for 24 h (A) or with 10 μM of each of these compounds for various time periods (B). At specified time points, MTT assays were performed. Results were normalized to values from the control cells at the initial time. All results were averaged from three independent studies.

As C_6-pyridinium ceramide treatment induces cell death as well as autophagy, we then examined whether inhibition or promotion of autophagy enhances cell survival. MCF7 cells were treated with the autophagy inhibitor 3-methyl adenine or the autophagy promoter tamoxifen, in the presence or absence of C_6-pyridinium ceramide for 24 h. Cells were then stained with Hoechst dye to detect apoptotic nuclei. As shown in **Fig. 5**, the presence of tamoxifen reduced the number of apoptotic nuclei following C_6-pyridinium ceramide treatment. This result suggests that in MCF7 cells, autophagy may serve as a protective mechanism against C_6-pyridinium ceramide-mediated mitochondrial damage.

C_6-pyridinium ceramide, but not C_6-ceramide, induces Bax translocation from the cytoplasm to mitochondria in MCF7 cells

C_6-pyridinium ceramide has been previously shown to be a potent anticancer agent that mediates mitochondrial permeabilization and cell death (23). Because Bax can induce mitochondrial permeabilization, we therefore set out to determine the role of this protein in C_6-pyridinium ceramide-mediated cell killing. A key step by which Bax promotes cell death involves its translocation from the cytoplasm to mitochondria (10, 11). In order to enable a rapid assessment of Bax subcellular localization, we used MCF7 breast carcinoma cell line stably expressing GFP-Bax (27).

Fluorescence microscopy analysis indicated that under nonapoptotic conditions, in greater than 98% of the cells Bax was localized to the cytoplasm and that in fewer than 2% of the cells Bax was localized to mitochondria. We found that when these cells were subjected to apoptosis induction with a variety of agents including the extrinsic pathway inducer TNF-α (10 ng/ml for 16 h), the intrinsic pathway inducer staurosporine (0.2 μM for 6 h), or C_6-pyridinium ceramide (10 μM for 16 h), there was a shift in the fluorescence pattern of GFP-Bax from a diffuse cytoplasmic state to a punctate membrane-bound state (**Fig. 6A**). On the other hand, GFP-Bax remained cytoplasmic in cells treated with C_6-ceramide or cetylpyridinium bromide (both, 10 μM for 16 h). To verify that punctate GFP-Bax localized with mitochondria, GFP-Bax-stable and Ds-red-mito-stable MCF7 cells were treated with C_6-ceramide or C_6-pyridinium ceramide and then visualized by fluorescence microscopy. As shown in Fig. 6B, punctate GFP-Bax colocalizes with DS-red-mito-labeled mitochondria. These results indicate that C_6-pyridinium ceramide, which localizes to mitochondria, induces Bax translocation to mitochondria.

To determine the time course of C_6-pyridinium ceramide-mediated Bax translocation to mitochondria, GFP-Bax-stable MCF7 cells were treated with 10 μM of this compound for various periods of time (**Fig. 7A**). We also treated cells with different concentrations of either C_6-ceramide or C_6-pyridinium ceramide for 18 h and quantitated the extent of GFP-Bax localization to mitochondria by fluorescence microscopy (Fig. 7B). Results showed that increasing concentrations of C_6-pyridinium ceramide

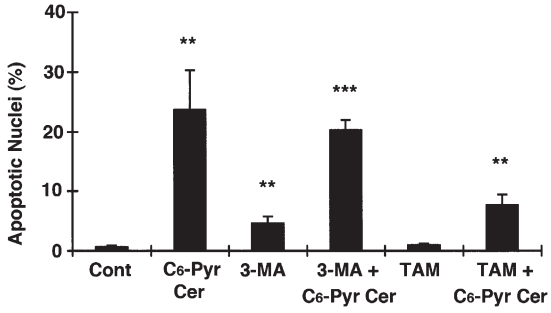

Fig. 5. Effect of autophagy regulators on C_6-pyridinium ceramide (C_6-Pyr-Cer)-mediated cell death. GFP-Bax-stable MCF7 cells were treated with or without 10 μM C_6-pyridinium ceramide either in the presence or absence of 40 μM tamoxifen (TAM) or 3 mM 3-methyl adenine (3-MA) for 24 h. Cells were then stained with Hoechst dye, and percentages of apoptotic nuclei were quantitated from three separate visual fields. Results were averaged from three independent studies. Values are means ± SEM. *, $P < 0.05$; **, $P < 0.01$; ***, $P < 0.001$ versus the control.

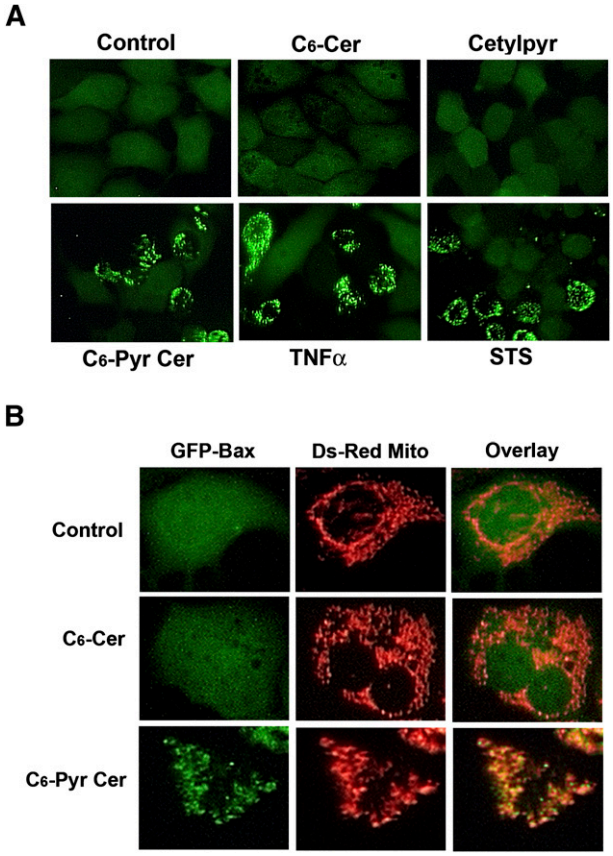

Fig. 6. C_6-pyridinium ceramide (C_6-Pyr-Cer) triggers Bax translocation from the cytoplasm to mitochondria in GFP-Bax-stable MCF7 cells. A: GFP-Bax-stable MCF7 cells were treated with 10 ng/ml TNF-α (18 h), 0.2 μM staurosporine (STS) (6 h), 10 μM C_6-ceramide (C_6-Cer), 10 μM cetylpyridinium bromide, or 10 μM C_6-pyridinium ceramide (18 h). Cells were then visualized by fluorescence microscopy. B: GFP-Bax and Ds-red-mito-stable (Ds-Red-Mito) MCF7 cells were treated with or without 10 μM C_6-ceramide or C_6-pyridinium ceramide (18 h) and then visualized by fluorescence microscopy. Fluorescence images from GFP (left panels) and Ds-red-mito (middle panels) are shown. Overlay of the two images is shown in the right panels.

increased the percentage of cells in which Bax was localized to mitochondria. On the other hand, we found that non-mitochondrion-targeting C_6-ceramide had little effect on promoting Bax translocation to mitochondria.

C_6-pyridinium ceramide induces Bax translocation from the cytoplasm to mitochondria via a caspase-dependent and Bid-independent manner

In order to examine the signaling pathway leading to Bax translocation to mitochondria in GFP-Bax-stable MCF7 cells treated with C_6-pyridinium ceramide, we first examined whether this translocation process was caspase dependent by the addition of the pan-caspase inhibitor zVAD-fmk. For verification of efficacy and specificity, cells were also treated with TNF-α or staurosporine in the presence or absence of zVAD-fmk. As shown in **Fig. 8A** and B, in the absence of zVAD-fmk, treatment with TNF-α resulted in approximately 90% of cells had Bax localized to mitochondria. In contrast, the percentage of GFP-Bax punctate cells in response to TNF-α was greatly reduced to 10% in the presence of zVAD-fmk, indicative of a direct role of caspase in TNF-α-mediated Bax translocation to mitochondria. On the other hand, the addition of zVAD-fmk had no effect on staurosporine-mediated Bax translocation. As for C_6-pyridinium ceramide, the addition of zVAD-fmk significantly decreased Bax translocation to mitochondria (Fig. 8A, B). In addition to using fluorescence microscopy, we carried out subcellular fractionation of control and treated cells. As shown in Fig. 8C, TNF-α, staurosporine, and C_6-pyridinium ceramide resulted in a shift in Bax (both GFP-tagged and endogenous) distribution from the cytosolic to mitochondrial fraction. Incubation of cells with zVAD-fmk significantly inhibited Bax redistribution to mitochondria in TNF-α- and C_6-pyridinium ceramide-treated cells. Therefore, caspases appear to be involved in the action of both agents on Bax.

To determine the role of Bid in C_6-pyridinium ceramide-mediated Bax translocation to mitochondria, GFP-Bax-stable MCF7 cells were treated with this compound either in the presence or absence of zVAD-fmk, and the treated cells were then subjected to immunofluorescence labeling with an anti-Bid antibody. For comparison, we also treated cells with 10 ng/ml TNF-α or 0.2 μM staurosporine. As shown in

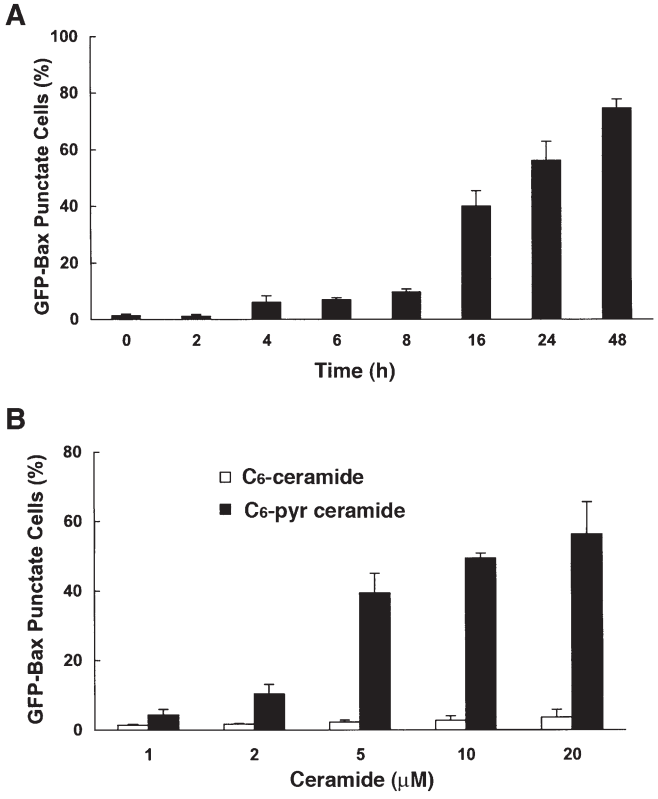

Fig. 7. Time course and dose effect analyses of C_6-pyridinium ceramide (C_6-Pyr-Cer)-mediated Bax translocation to mitochondria. A: GFP-Bax-stable MCF7 cells were treated with 10 μM C_6-pyridinium ceramide for 2, 4, 6, 8, 16, 24, and 48 h. Percentages of GFP-Bax punctate cells were quantitated from four separate visual fields. B: GFP-Bax-stable MCF7 cells were treated with various concentrations of C_6-ceramide (C_6-Cer) or C_6-pyridinium ceramide for 16 h. Percentages of GFP-Bax punctate cells were quantitated from four separate visual fields. Results were averaged from three independent studies. Error bars represent SDs.

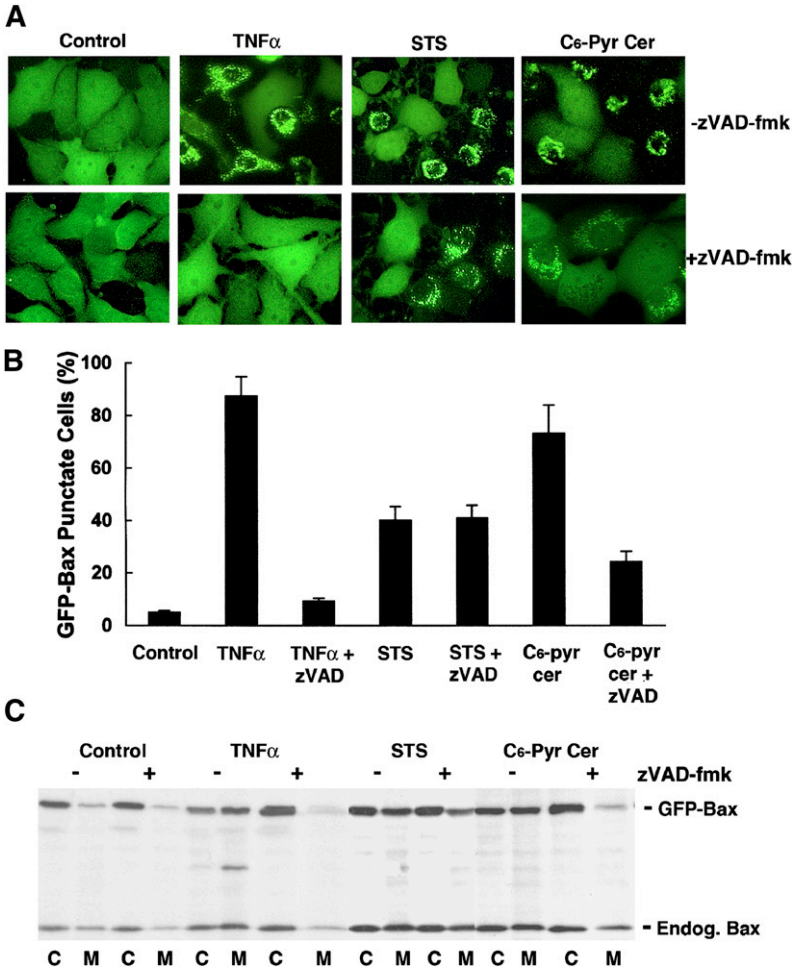

Fig. 8. C_6-pyridinium ceramide (C_6-Pyr-Cer)-induced Bax translocation to mitochondria is partially inhibited by zVAD-fmk. A: GFP-Bax-stable MCF7 cells were treated with 10 ng/ml TNF-α (16 h), 0.2 μM staurosporine (6 h), or 20 μM C_6-pyridinium ceramide (16 h) either in the absence or presence of 50 μM zVAD-fmk. Cells were visualized by fluorescence microscopy. B: A quantitative analysis of the effect of zVAD-fmk on regulation of TNF-α, staurosporine (STS), and C_6-pyridinium ceramide-mediated Bax translocation to mitochondria. Percentages of cells having GFP-Bax localized to mitochondria were averaged from three separate visual fields. The study was carried out three times. C: MCF7 cells stably expressing GFP-Bax were treated with the above-stated compounds. Treated cells were then separated into soluble protein (C) and heavy membrane (M) fractions. Protein samples were analyzed by Western blotting with an anti-Bax antibody.

Fig. 9A, for cells treated with TNF-α in the absence of zVAD-fmk, Bid colocalized with mitochondrially bound Bax. Addition of zVAD-fmk, which blocked Bax translocation to mitochondria, also resulted in a cytoplasmic Bid localization pattern. Treatment with either staurosporine or C_6-pyridinium ceramide resulted in GFP-Bax localization to mitochondria, while Bid remained in the cytoplasm, and this localization pattern was independent of zVAD-fmk addition.

In order to corroborate immunofluorescence labeling assays, Western blotting analysis of cell lysates was performed with an anti-Bid antibody to detect Bid cleavage. As shown in Fig. 9B, treatment with TNF-α resulted in Bid cleavage in a caspase-dependent manner, in agreement with previous reports (29, 30). No Bid cleavage, however, was observed in staurosporine- or C_6-pyridinium ceramide-treated cells.

To ascertain that Bid is not involved in C_6-pyridinium ceramide-mediated Bax translocation to mitochondria, GFP-Bax-stable MCF7 cells were transfected with Bid siRNA oligonucleotides to knockdown the expression level of this protein. As shown in Fig. 9C, treatment with Bid siRNA knocked down Bid protein level without affecting the expression levels of other cellular proteins including Bcl-2 and ATP synthase β-subunit. Both scrambled and Bid siRNA oligonucleotide-transfected cells were treated with TNF-α, staurosporine, or C_6-pyridinium ceramide. Figure 9D shows that whereas Bid knockdown affected TNF-α-mediated Bax translocation to mitochondria, it had no effect on staurosporine- or C_6-pyridinium ceramide-mediated Bax redistribution. Overall, these results indicate that C_6-pyridinium ceramide-mediated Bax translocation to mitochondria in MCF7 cells is dependent on a caspase but independent of Bid.

C_6-pyridinium ceramide-induced Bax translocation leads to cytochrome c release and cell death

Previously, it has been shown that Bax translocation to mitochondria leads to the release of cytochrome c (14, 31, 32) and cell death. By using immunofluorescence labeling with an anti-cytochrome c antibody, we found that in healthy cells, where GFP-Bax was cytoplasmic, cytochrome c was retained in mitochondria (**Fig. 10A**). On the other hand, cytoplasmic cytochrome c became evident in TNF-α-, staurosporine-, and C_6-pyridinium ceramide-treated cells that had GFP-Bax localized to mitochondria. In addition, by staining both the untreated and treated cells with Hoechst nuclear stain, we found that there was significant cell death, as evidenced by nuclear condensation in cells that had GFP-Bax localized to mitochondria (Fig. 10B). These results indicate that C_6-pyridinium ceramide-induced mitochondrial permeabilization and cell death involve Bax.

DISCUSSION

C_6-pyridinium ceramide was developed as a positively charged ceramide that preferentially accumulates in mi-

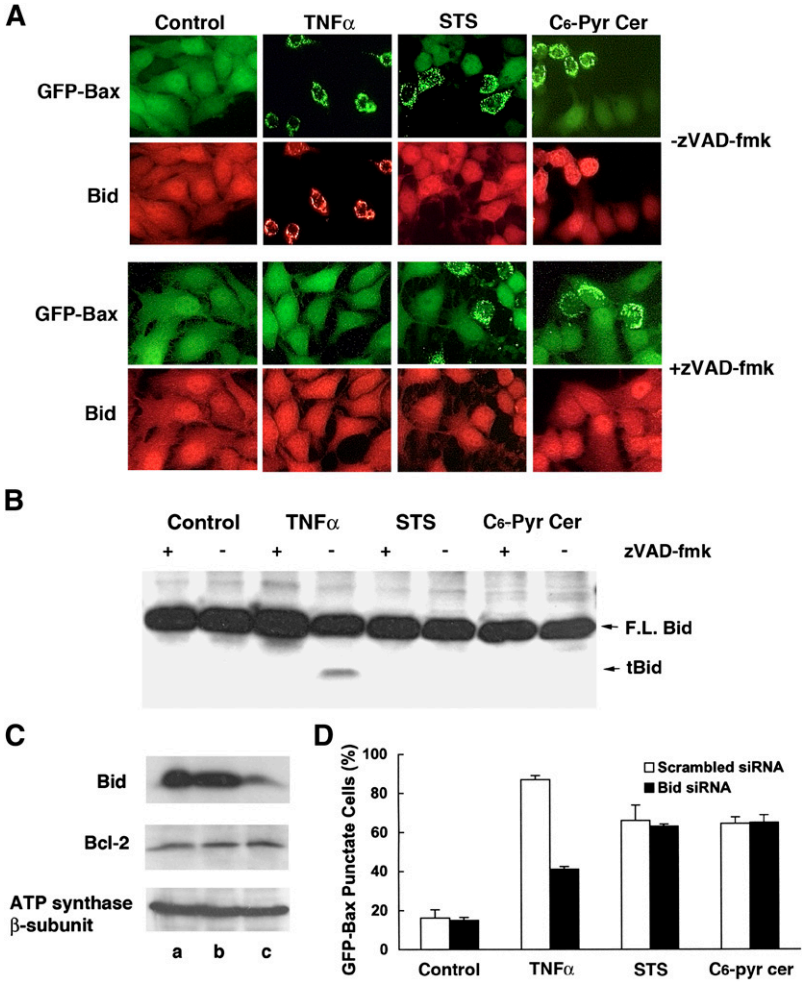

Fig. 9. Bid is not involved in C_6-pyridinium ceramide-(C_6-Pyr-Cer) mediated Bax translocation to mitochondria. A: MCF7 cells stably expressing GFP-Bax were treated with 10 ng/ml TNF-α (18 h), 0.2 μM staurosporine (STS) (6 h), or 10 μM C_6-pyridinium ceramide (18 h) either in the absence or presence of zVAD-fmk. Cells were then subjected to immunofluorescence labeling with an anti-Bid antibody. Labeled cells were visualized by fluorescence microscopy. B: GFP-Bax-stable MCF7 cells were treated with various apoptosis inducing agents (TNF-α, staurosporine, C_6-pyridinium ceramide) in the presence or absence of zVAD-fmk. Cell lysates prepared from untreated and treated cells were analyzed by Western blotting with an anti-Bid antibody. C: GFP-Bax-stable MCF7 cells were transfected with either scrambled, nonsilencing siRNA or Bid siRNA oligonucleotides for 64 h. Cell lysates from untransfected (lane a), scrambled siRNA (lane b), and Bid siRNA (lane c) oligonucleotide transfected cells were then analyzed by Western blotting with anti-Bid, Bcl-2, and ATP synthase β-subunit antibodies. D. MCF7 cells stably expressing GFP-Bax were transfected with either scrambled siRNA or Bid siRNA oligonucleotide for 48 h. Cells were then treated with 10 ng/ml TNF-α (18 h), 0.2 μM staurosporine (6 h), or 10 μM C_6-pyridinium ceramide (18 h). Cells were subsequently visualized by fluorescence microscopy and the percentages of GFP-Bax punctate cells were quantitated from four separate visual fields. The study was carried out three times.

tochondria of living cells (23). In this report, we compared the biological effects of this mitochondrion-targeting C_6-ceramidoid to its neutral non-mitochondrion-targeting analog. We found that this positively charged ceramide preferentially promotes cellular autophagy, retards cell growth, and induces cellular apoptosis.

Short-chained ceramides have been shown to promote cellular autophagy (5). In the current study, we show that

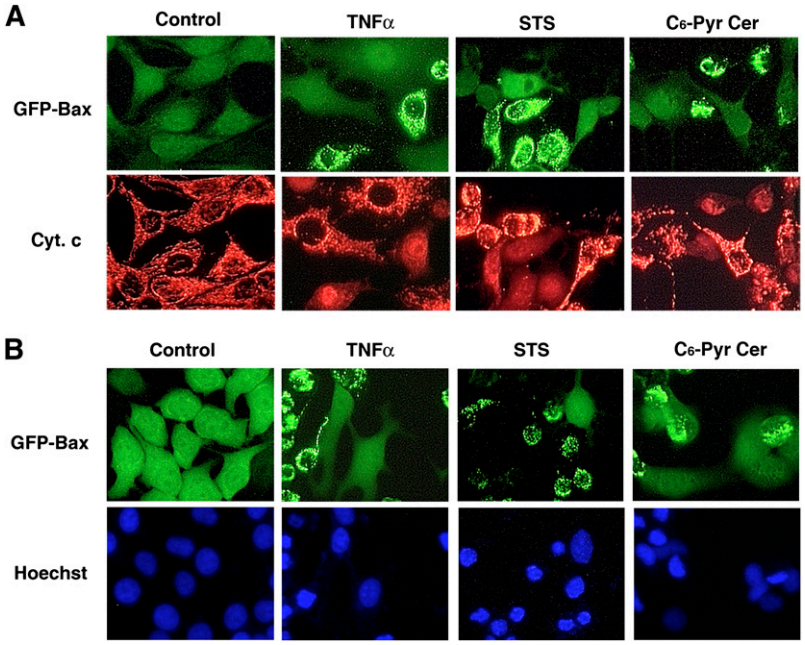

Fig. 10. Bax localization to mitochondria in GFP-Bax-stable MCF7 cells is associated with the release of cytochrome c (Cyt. c) and nuclear condensation. A: GFP-Bax-stable MCF7 cells were treated with 10 ng/ml TNF-α (18 h), 0.2 μM staurosporine (STS) (6 h), or 10 μM C_6-pyridinium ceramide (C_6-Pyr-Cer) (18 h). Untreated and treated cells were then subjected to immunofluorescence labeling with an anti-cytochrome c antibody and visualized by fluorescence microscopy. B: GFP-Bax-stable MCF7 cells were treated with the above-stated apoptotic stimuli. Cells were then stained with Hoechst nuclear stain and visualized by fluorescence microscopy.

C_6-pyridinium ceramide treatment of MCF7 cells significantly enhanced the production of acidic vesicular organelles and autophagosomes and elevated the level of LC3-II. On the other hand, no significant formation of acidic vesicular organelles, autophagosomes, or LC3-II was observed in C_6-ceramide-treated MCF7 cells. Interestingly, formation of LC3-II was observed in MDA-MB-231 cells treated with C_6-ceramide. This suggests that the formation of autophagosomes induced by short-chained ceramide may be cell-type dependent. Moreover, upregulation of Beclin-1 has been suggested as a mechanism by which ceramide promotes autophagy (5). However, in our study, we did not observe a ceramide-induced elevation in Beclin-1. Alternatively, it is possible that ceramide may enhance JNK1-depedent Bcl-2 phosphorylation to enable its dissociation from Beclin-1 to promote autophagy (33).

Autophagy has been proposed to act either as a tumor suppressor to promote cancer cell death or as a cytoprotective mechanism to shield cancer cells against anticancer treatments (34). In our study, we found that treatment of MCF7 cells with the autophagy promoter tamoxifen could attenuate C_6-pyridinium ceramide-mediated cell death, suggesting that autophagy may represent a cellular protective mechanism. In addition, we found that this compound induced autophagy within the same time frame as apoptotic cell death in MCF7 cells. In our study, we found that the pan-caspase inhibitor zVAD-fmk could attenuate C_6-pyridinium ceramide-mediated Bax redistribution and cell death but not autophagosome formation (data not shown). Either these two events are independent of each other or autophagosome formation is upstream of the zVAD-fmk-sensitive portion of the Bax-activation signaling pathway. Interestingly, Akt activation has been shown to suppress apoptosis and autophagy (35, 36), and a ceramide could suppress Akt activity though activation of protein phosphatase 2 (37, 38). It is possible that C_6-pyridinium ceramide could more effectively activate protein phosphatase 2 than C_6-ceramide to promote both apoptosis and autophagy.

Previously, it has been reported that C_6-pyridinium ceramide can attenuate the proliferation of resting T cells (4). In the current study, it was shown that C_6-pyridinium ceramide could greatly reduce the rate of cell growth compared with its uncharged analog in breast epithelial and breast cancer cell lines, with higher IC_{50} values in breast epithelial cells than in cancer cells. The accumulation of C_6-pyridinium ceramide in mitochondria and its ability to promote mitochondrial permeabilization (23) likely reduced mitochondrial function and cell viability, thus contributing to the observed decrease in the rate of cell growth.

Currently, two main apoptotic signaling pathways have been proposed that regulate Bax translocation to mitochondria. In the extrinsic pathway of apoptosis, caspase-8-cleaved Bid activates Bax and leads to Bax translocation to mitochondria. On the other hand, in the intrinsic pathway of apoptosis, Bax activation and mitochondrial translocation are independent of caspase-8 and Bid. In this study, we have uncovered a unique Bax-activating process mediated by C_6-pyridinium ceramide in MCF7 cells that is dependent on a caspase but independent of Bid.

Previously, it was reported that C_6-pyridinium ceramide could induce mitochondrial permeabilization (23). Based on the current study, it is likely that this permeabilization is mediated through Bax translocation to mitochondria, causing the release of apoptogenic proteins such as cytochrome c. In addition, it has been shown that addition of C_2- and C_6-ceramide could cause a Bax conformational change and localization to mitochondria (16, 39–41). Fluorescently labeled short-chain ceramide species have been shown to be localized to the Golgi apparatus (23, 42). Surprisingly, in our study, we found that C_6-ceramide had little effect in triggering Bax translocation, even at high concentrations. This difference may be due to the different cell types used and the method of detecting Bax translocation. Alternatively, it may be possible that C_6-ceramide also reaches mitochondria; however, the local concentrations are either lower or it is metabolized differently than C_6-pyridinium ceramide. Interestingly, we found that addition of cetylpyridinium bromide did not promote Bax translocation, suggesting that the pyridinium moiety of the C_6-pyridinium ceramide, although important for targeting to mitochondria, is not responsible for Bax activation.

It was recently reported that D-*erythro*-sphingosine could promote Bax activation in rhabdomyosarcoma cells (43). This effect appeared to be stereo-specific as its L-*erythro* and DL-*threo* analogs were ineffective at inducing cell death. We have tested L-*erythro*- and L-*threo*-C_6-pyridinium ceramides (LCL187 and LCL124, respectively) and found them to be equally effective at triggering Bax translocation to mitochondria (Hou et al., unpublished data). This suggests that stereochemistry of C_6-pyridinium ceramide is not critical in regulating Bax translocation.

Bax undergoes a conformational change as it redistributes to mitochondria (44). It has been previously shown that Bax conformational change could be induced by nonionic detergents (9, 28). In our study, we found that incubation of soluble Bax with C_6-pyridinium ceramide did not lead to a conformational change (Hou and Hsu, data not shown). This suggests that Bax activation is a consequence of the signaling event initiated by this mitochondrion-targeting ceramide rather than a direct alteration of Bax conformation by this compound.

In the TNF-α-mediated apoptotic pathway, activation of caspase-8 causes Bid cleavage. tBid then translocates to mitochondria and activates Bax. In our GFP-Bax-stable MCF7 cells, we also observed this TNF-α-mediated Bid cleavage and the cotranslocation of Bid and Bax to mitochondria. This is in contrast with the staurosporine-induced apoptotic pathway in which we observed Bax translocation to mitochondria in the absence of Bid cleavage and mitochondrial translocation. On the other hand, we found that C_6-pyridinium ceramide triggered Bax translocation to mitochondria via a caspase-dependent pathway but without Bid cleavage and without colocalization to mitochondria. Consistently, we found that knockdown of Bid by the siRNA approach attenuated Bax translocation in TNF-α- but not in staurosporine- or C_6-pyridinium ceramide-treated cells.

TNF-α has been previously shown to elevate ceramide production in HL-60 and A431 cells (45, 46). It remains to be determined to what extent this elevated pool of ceramide contributes to Bax activation.

It has been reported that ceramides derived from acid sphingomyelinase in the lysosome could activate cathepsin D (47), which in turn, could lead to Bax activation by an as-yet-unknown mechanism (48). We found that pepstatin A, which has been reported to inhibit cathepsin D and Bax activation in staurosporine-treated T lymphocytes, had no effect in influencing Bax localization in C_6-pyridinium ceramide- or staurosporine-treated MCF7 cells (Hou and Hsu, unpublished observation). This suggests that Bax translocation induced by C_6-pyridinium ceramide in MCF7 cells likely does not involve cathepsin D and may be distinct from the lysosomal pathways mediated by ceramide.

In MCF7 cells, we found that C_6-pyridinium ceramide-mediated Bax redistribution appeared to be caspase-dependent. Further analysis with various caspase inhibitors indicated that the caspase-5 inhibitor z-WEHD-fmk could also significantly inhibit Bax redistribution (Hou and Hsu, unpublished data). Although this caspase-dependent signaling pathway appeared to be important for Bax redistribution, it is unique, however, only to MCF7 cells. We found that in DU-145, NT-2, LS-180, and DLD cells stably expressing GFP-Bax, addition of zVAD-fmk did not attenuate C_6-pyridinium ceramide-mediated Bax redistribution (Hou and Hsu, unpublished data).

Overall, our study shows that selective compartmentalization of ceramide may affect the potency of this signaling molecule in regulating various cellular processes. This is evidenced by differential regulations of cellular autophagy, growth, and viability that are elicited by mitochondrion- and non-mitochondrion-targeting ceramide species. It will be interesting in the future to identify the direct molecular targets of C_6-pyridinium ceramide that facilitate the regulation of the above-stated biological processes.

REFERENCES

1. Bartke, N., and Y. A. Hannun. 2009. Bioactive sphingolipids: metabolism and function. *J. Lipid Res.* **50**(Suppl): S91–S96.
2. Ruvolo, P. P. 2003. Intracellular signal transduction pathways activated by ceramide and its metabolites. *Pharmacol. Res.* **47:** 383–392.
3. Zheng, W., J. Kollmeyer, H. Symolon, A. Momin, E. Munter, E. Wang, S. Kelly, J. C. Allegood, Y. Liu, Q. Peng, et al. 2006. Ceramides and other bioactive sphingolipid backbones in health and disease: lipidomic analysis, metabolism and roles in membrane structure, dynamics, signaling and autophagy. *Biochim. Biophys. Acta.* **1758:** 1864–1884.
4. O'Byrne, D., and D. Sansom. 2000. Lack of costimulation by both sphingomyelinase and C2 ceramide in resting human T cells. *Immunology.* **100:** 225–230.
5. Scarlatti, F., C. Bauvy, A. Ventruti, G. Sala, F. Cluzeaud, A. Vandewalle, R. Ghidoni, and P. Codogno. 2004. Ceramide-mediated macroautophagy involves inhibition of protein kinase B and up-regulation of beclin 1. *J. Biol. Chem.* **279:** 18384–18391.
6. Obeid, L. M., C. M. Linardic, L. A. Karolak, and Y. A. Hannun. 1993. Programmed cell death induced by ceramide. *Science.* **259:** 1769–1771.
7. Oltvai, Z. N., C. L. Milliman, and S. J. Korsmeyer. 1993. Bcl-2 heterodimerizes in vivo with a conserved homolog, Bax, that accelerates programmed cell death. *Cell.* **74:** 609–619.
8. Hsu, Y-T., K. G. Wolter, and R. J. Youle. 1997. Cytosol-to-membrane redistribution of Bax and Bcl-XL during apoptosis. *Proc. Natl. Acad. Sci. U S A.* **94:** 3668–3672.
9. Hsu, Y-T., and R. J. Youle. 1998. Bax in murine thymus is a soluble monomeric protein that displays differential detergent-induced conformations. *J. Biol. Chem.* **273:** 10777–10783.
10. Wolter, K. G., Y-T. Hsu, C. L. Smith, A. Nechushtan, X-G. Xi, and R. J. Youle. 1997. Movement of Bax from the cytosol to mitochondria during apoptosis. *J. Cell Biol.* **139:** 1281–1292.
11. Gross, A., J. Jockel, M. C. Wei, and S. J. Korsmeyer. 1998. Enforced dimerization of Bax results in its translocation, mitochondrial dysfunction and apoptosis. *EMBO J.* **17:** 3878–3885.
12. Smaili, S. S., Y-T. Hsu, K. M. Sanders, J. T. Russell, and R. J. Youle. 2001. Bax translocation to mitochondria subsequent to a rapid loss of mitochondrial membrane potential. *Cell Death Differ.* **8:** 909–920.
13. DiGiorgi, F., L. Lartigue, M. K. Bauer, A. Schubert, S. Grimm, G. T. Hanson, S. J. Remington, R. J. Youle, and F. Ichas. 2002. The permeability transition pore signals apoptosis by directing Bax translocation and multimerization. *FASEB J.* **16:** 607–609.
14. Manon, S., B. Chaudhuri, and M. Guerin. 1997. Release of cytochrome c and decrease of cytochrome c oxidase in Bax-expressing yeast cells, and prevention of these effects by coexpression of Bcl-XL. *FEBS Lett.* **415:** 29–32.
15. Eskes, R., B. Antonsson, A. Osen-Sand, S. Montessuit, C. Richter, R. Sadoul, G. Mazzei, A. Nichols, and J-C. Martinou. 1998. Bax-induced cytochrome c release from mitochondria is independent of the permeability transition pore but highly dependent on Mg2+ ions. *J. Cell Biol.* **143:** 217–224.
16. Kim, H. J., J. Y. Mun, Y. J. Chun, K. H. Choi, and M. Y. Kim. 2001. Bax-dependent apoptosis induced by ceramide in HL-60 cells. *FEBS Lett.* **505:** 264–268.
17. Kashkar, H., K. Wiegmann, B. Yazdanpanah, D. Haubert, and M. Kronke. 2005. Acid sphingomyelinase is indispensable for UV light-induced Bax conformational change at the mitochondrial membrane. *J. Biol. Chem.* **280:** 20804–20813.
18. Birbes, H., C. Luberto, Y. T. Hsu, S. E. Bawab, Y. A. Hannun, and L. M. Obeid. 2005. A mitochondrial pool of sphingomyelin is involved in TNFalpha-induced Bax translocation to mitochondria. *Biochem. J.* **386:** 445–451.
19. Putcha, G. V., C. A. Harris, K. L. Moulder, R. M. Easton, C. B. Thompson, and E. M. Johnson, Jr. 2002. Intrinsic and extrinsic pathway signaling during neuronal apoptosis: lessons from the analysis of mutant mice. *J. Cell Biol.* **157:** 441–453.
20. Desagher, S., A. Osen-Sand, A. Nichols, R. Eskes, S. Montessuit, S. Lauper, K. Maundrell, B. Antonsson, and J. C. Martinou. 1999. Bid-induced conformational change of Bax is responsible for mitochondrial cytochrome c release during apoptosis. *J. Cell Biol.* **144:** 891–901.
21. Eskes, R., S. Desagher, B. Antonsson, and J. C. Martinou. 2000. Bid induces the oligomerization and insertion of Bax into the outer mitochondrial membrane. *Mol. Cell. Biol.* **20:** 929–935.
22. Perez, D., and E. White. 2000. TNF-alpha signals apoptosis through a bid-dependent conformational change in Bax that is inhibited by E1B 19K. *Mol. Cell.* **6:** 53–63.
23. Novgorodov, S. A., Z. M. Szulc, C. Luberto, J. A. Jones, J. Bielawski, A. Bielawska, Y. A. Hannun, and L. M. Obeid. 2005. Positively charged ceramide is a potent inducer of mitochondrial permeabilization. *J. Biol. Chem.* **280:** 16096–16105.
24. Szulc, Z. M., J. Bielawski, H. Gracz, M. Gustilo, N. Mayroo, Y. A. Hannun, L. M. Obeid, and A. Bielawska. 2006. Tailoring structure–function and targeting properties of ceramides by site-specific cationization. *Bioorg. Med. Chem.* **14:** 7083–7104.
25. Senkal, C. E., S. Ponnusamy, M. J. Rossi, K. Sundararaj, Z. Szulc, J. Bielawski, A. Bielawska, M. Meyer, B. Cobanoglu, S. Koybasi, et al. 2006. Potent antitumor activity of a novel cationic pyridinium-ceramide alone or in combination with gemcitabine against human head and neck squamous cell carcinomas in vitro and in vivo. *J. Pharmacol. Exp. Ther.* **317:** 1188–1199.
26. Rossi, M. J., K. Sundararaj, S. Koybasi, M. S. Phillips, Z. M. Szulc, A. Bielawska, T. A. Day, L. M. Obeid, Y. A. Hannun, and B. Ogretmen. 2005. Inhibition of growth and telomerase activity by novel cationic ceramide analogs with high solubility in human head and neck squamous cell carcinoma cells. *Otolaryngol. Head Neck Surg.* **132:** 55–62.
27. Jin, J., T. D. Mullen, Q. Hou, J. Bielawski, A. Bielawska, X. Zhang, L. M. Obeid, Y. A. Hannun, and Y. T. Hsu. 2009. AMPK inhibi-

tor Compound C stimulates ceramide production and promotes Bax redistribution and apoptosis in MCF7 breast carcinoma cells. *J. Lipid Res.* **50:** 2389–2397.
28. Hsu, Y-T., and R. J. Youle. 1997. Nonionic detergents induce dimerization among members of the Bcl-2 family. *J. Biol. Chem.* **272:** 13829–13834.
29. Luo, X., I. Budihardjo, H. Zou, C. Slaughter, and X. Wang. 1998. Bid, a Bcl-2 interacting protein, mediates cytochrome c release from mitochondria in response to activation of cell surface death receptors. *Cell.* **94:** 481–490.
30. Gross, A., X. M. Yin, K. Wang, M. C. Wei, J. Jockel, C. Milliman, H. Erdjument-Bromage, P. Tempst, and S. J. Korsmeyer. 1999. Caspase cleaved BID targets mitochondria and is required for cytochrome c release, while BCL-XL prevents this release but not tumor necrosis factor-R1/Fas death. *J. Biol. Chem.* **274:** 1156–1163.
31. Antonsson, B., S. Montessuit, B. Sanchez, and J. C. Martinou. 2001. Bax is present as a high molecular weight oligomer-complex in the mitochondrial membrane of apoptotic cells. *J. Biol. Chem.* **276:** 11615–11623.
32. Mikhailov, V., M. Mikhailova, D. J. Pulkrabek, Z. Dong, M. A. Venkatachalam, and P. Saikumar. 2001. Bcl-2 prevents Bax oligomerization in the mitochondrial outer membrane. *J. Biol. Chem.* **276:** 18361–18374.
33. Pattingre, S., C. Bauvy, S. Carpentier, T. Levade, B. Levine, and P. Codogno. 2009. Role of JNK1-dependent Bcl-2 phosphorylation in ceramide-induced macroautophagy. *J. Biol. Chem.* **284:** 2719–2728.
34. Li, D. D., L. L. Wang, R. Deng, J. Tang, Y. Shen, J. F. Guo, Y. Wang, L. P. Xia, G. K. Feng, Q. Q. Liu, et al. 2009. The pivotal role of c-Jun NH2-terminal kinase-mediated Beclin 1 expression during anticancer agents-induced autophagy in cancer cells. *Oncogene.* **28:** 886–898.
35. Dudek, H., S. R. Datta, T. F. Franke, M. J. Birnbaum, R. Yao, G. M. Cooper, R. A. Segal, D. R. Kaplan, and M. E. Greenberg. 1997. Regulation of neuronal survival by the serine-threonine protein kinase Akt. *Science.* **275:** 661–665.
36. Arico, S., A. Petiot, C. Bauvy, P. F. Dubbelhuis, A. J. Meijer, P. Codogno, and E. Ogier-Denis. 2001. The tumor suppressor PTEN positively regulates macroautophagy by inhibiting the phosphatidylinositol 3-kinase/protein kinase B pathway. *J. Biol. Chem.* **276:** 35243–35246.
37. Zhou, H., S. A. Summers, M. J. Birnbaum, and R. N. Pittman. 1998. Inhibition of Akt kinase by cell-permeable ceramide and its implications for ceramide-induced apoptosis. *J. Biol. Chem.* **273:** 16568–16575.
38. Schubert, K. M., M. P. Scheid, and V. Duronio. 2000. Ceramide inhibits protein kinase B/Akt by promoting dephosphorylation of serine 473. *J. Biol. Chem.* **275:** 13330–13335.
39. Belaud-Rotureau, M. A., N. Leducq, F. M. P. d. Gannes, P. Diolez, L. Lacoste, F. Lacombe, P. Bernard, and F. Belloc. 2000. Early transitory rise in intracellular pH leads to Bax conformation change during ceramide-induced apoptosis. *Apoptosis.* **5:** 551–560.
40. von Haefen, C., T. Wieder, B. Gillissen, L. Starck, V. Graupner, B. Dorken, and P. T. Daniel. 2002. Ceramide induces mitochondrial activation and apoptosis via a Bax-dependent pathway in human carcinoma cells. *Oncogene.* **21:** 4009–4019.
41. Xin, M., and X. Deng. 2006. Protein phosphatase 2A enhances the proapoptotic function of Bax through dephosphorylation. *J. Biol. Chem.* **281:** 18859–18867.
42. Hu, W., R. Xu, G. Zhang, J. Jin, Z. M. Szulc, J. Bielawski, Y. A. Hannun, L. M. Obeid, and C. Mao. 2005. Golgi fragmentation is associated with ceramide-induced cellular effects. *Mol. Biol. Cell.* **16:** 1555–1567.
43. Phillips, D. C., S. Martin, B. T. Doyle, and J. A. Houghton. 2007. Sphingosine-induced apoptosis in rhabdomyosarcoma cell lines is dependent on pre-mitochondrial Bax activation and post-mitochondrial caspases. *Cancer Res.* **67:** 756–764.
44. Nechushtan, A., C. L. Smith, Y-T. Hsu, and R. J. Youle. 1999. Conformation of the Bax C-terminus regulates subcellular location and cell death. *EMBO J.* **18:** 2330–2341.
45. Kim, M. Y., C. Linardic, L. Obeid, and Y. Hannun. 1991. Identification of sphingomyelin turnover as an effector mechanism for the action of tumor necrosis factor alpha and gamma-interferon. Specific role in cell differentiation. *J. Biol. Chem.* **266:** 484–489.
46. Mathias, S., K. A. Dressler, and R. N. Kolesnick. 1991. Characterization of a ceramide-activated protein kinase: stimulation by tumor necrosis factor alpha. *Proc. Natl. Acad. Sci. U S A.* **88:** 10009–10013.
47. Heinrich, M., M. Wickel, W. Schneider-Brachert, C. Sandberg, J. Gahr, R. Schwandner, T. Weber, P. Saftig, C. Peters, J. Brunner, M. Kronke, and S. Schutze. 1999. Cathepsin D targeted by acid sphingomyelinase-derived ceramide. *EMBO J.* **18:** 5252–5263.
48. Bidere, N., H. K. Lorenzo, S. Carmona, M. Laforge, F. Harper, C. Dumont, and A. Senik. 2003. Cathepsin D triggers Bax activation, resulting in selective apoptosis-inducing factor (AIF) relocation in T lymphocytes entering the early commitment phase to apoptosis. *J. Biol. Chem.* **278:** 31401–31411.